Inorg. Chem. **2003**, *42*, 541–551

Molecular, 1D, and 2D Systems Built from Phenylcyanamido Ligands. Syntheses, Crystal Structures, and Characterization of Their Magnetic Properties

Albert Escuer,*,† Núria Sanz,† Ramon Vicente,† and Franz A. Mautner‡

Departament de Química Inorgànica, Universitat de Barcelona, c/ Martí Franqués 1-11, 08028 Barcelona, Spain, and Institut für Physikalische und Theoretische Chemie, Technische Universität Graz, A-8010 Graz, Austria

Received August 6, 2002

Several Mn^{II} compounds with phenylcyanamido ligands have been synthesized and characterized by means of single-crystal X-ray structural determination. The reported compounds show a wide variety of nuclearity from mononuclear and dinuclear systems to 1D chains and 2D networks in which X-phenylcyanamide (X-pcyd) anions act as the bridging ligand. Mononuclear compound $[Mn(H_2O)_2(4\text{-bzpy})_2(3\text{-Cl-pcyd})_2]$ (**1**) crystallizes in the monoclinic system, *P*21/*a* space group, dinuclear compounds $(\mu_{1,3}\text{-3-Cl-pcyd})_2[Mn(2,2'\text{-bpy})(3\text{-Cl-pcyd})(MeOH)]_2$ (**2**) and $(\mu_{1,3}\text{-3-Cl-pcyd})_2[Mn(2,2'\text{-bpy})(3\text{-Cl-pcyd})(EtOH)]_2$ (**3**) crystallize in the triclinic system, $P\bar{1}$ space group, 1D chain $\{(\mu_{1,3}\text{-4-Cl-pcyd})_2[Mn(2,2'\text{-bpy})]\}_n$ (**4**) crystallizes in the monoclinic system, *I*2/*a* space group, and 2D network $[Mn(\mu\text{-4,4'-bpy})(\mu_{1,3}\text{-3-F-pcyd})_2]_n$ (**5**) crystallizes in the monoclinic system, *C*2 space group. Susceptibility measurements on compounds **2**–**4** reveal moderate antiferromagnetic coupling in all cases. MO calculations have been made to elucidate the main factors that control the superexchange pathway for this kind of ligand. Comparison of their magnetic behavior with that of related ligands such as azido and dicyanamido is reported.

Introduction

Work on polynuclear systems derived from azide[1] or dicyanamide[2] (dca) anions acting as bridging ligands is a fast-growing research field due to the large variety of topologies, dimensionalities, and magnetic properties that can be obtained. Dicyanamide may act as a bidentate ligand by coordination to two different metallic centers by means of the terminal nitrile N-atoms ($\mu_{1,5}$ mode) or as a tridentate ligand giving a variety of rutile-like 3D $[M(dca)_2]$ compounds by means of the additional coordination of the central amide N-atom[3] ($\mu_{1,3,5}$ mode). Azido ligand also frequently shows two main coordination modes. One of these modes uses the two terminal N-atoms ($\mu_{1,3}$ mode), but a $\mu_{1,1}$ mode also occurs in which only one N-atom coordinates two metallic ions.[1] Other exotic modes involving coordination to three[4] or even four[5] metallic ions have been reported. From the magnetic point of view, azido ligand is able to transmit strong ferromagnetic (F) or antiferromagnetic (AF) interactions, depending on the coordination mode,[1] whereas dca derivatives are always weakly coupled.[6]

In contrast, much less is known about the phenylcyanamido (pcyd) ligands, despite the formal similarities with the azido or dca ligands, Chart 1. The triatomic −NCN group is electronically similar to the azido ligand, and similar coordination modes may be reasonably expected. On the other hand, the nitrile group approaches the coordination properties of the dca ligand (mainly for M−N−C and M−N bond parameters).

* Author to whom correspondence should be addressed. E-mail: albert.escuer@qi.ub.es.

† Universitat de Barcelona.

‡ Technische Universität Graz.

(1) Ribas, J.; Escuer, A.; Monfort, M.; Vicente, R.; Cortés, R.; Lezama, L.; Rojo, T. *Coord. Chem. Rev.* **1999**, *193*−*195*, 1027.

(2) Van der Werff, P. M.; Batten, S. R.; Jensen, P.; Moubaraki, B.; Murray, K. S. *Inorg. Chem.* **2001**, *40*, 1718. Raebiger, J. W.; Manson, J. L.; Sommer, R. D.; Geiser, U.; Rheingold, A. L.; Miller, J. S. *Inorg. Chem.* **2001**, *40*, 2578. Vangdal, B.; Carranza, J.; Lloret, F.; Julve, M.; Sletten, J. *J. Chem. Soc., Dalton Trans.* **2002**, 566 and references therein.

(3) Manson, J. L.; Kmety, C. R.; Epstein, A. J.; Miller, J. S. *Inorg. Chem.* **1999**, *38*, 2552. Batten, S. R.; Harris, A. R.; Jensen, P.; Murray, K. S.; Ziebell, A. *J. Chem. Soc., Dalton Trans.* **2000**, 3829. Kutasi, A. M.; Batten, S. R.; Moubaraki, B.; Murray, K. S. *J. Chem. Soc., Dalton Trans.* **2002**, 819 and references therein.

(4) Goher, M. A. S.; Cano, J.; Journaux, Y.; Abu-Youssef, M. A. M.; Mautner, F. A.; Escuer, A.; Vicente, R. *Chem.*−*Eur. J.* **2000**, *6*, 778.

(5) Papaefstathiou, G. S.; Perlepes, S. P.; Escuer, A.; Vicente, R.; Font-Bardia, M.; Solans, X. *Angew. Chem.* **2001**, *113*, 908; *Angew. Chem., Int. Ed.* **2001**, *40*, 884.

(6) Escuer, A.; Sanz, N.; Mautner, F. A.; Vicente, R. *Inorg. Chem.* **2000**, *39*, 1668.

10.1021/ic025931l CCC: $25.00
Published on Web 12/24/2002

Chart 1

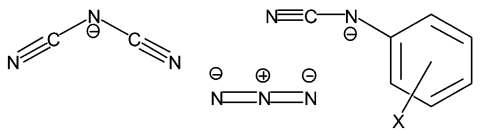

This intermediate position between the azido and dca ligands also appears in regard to the MO involved in the superexchange interaction for each ligand. Azide ion has two efficient nonbonding orthogonal π orbitals, whereas dca ligand has one π and one σ orbital, a much less efficient superexchange pathway due to the low contribution of nitrile N-atoms and the shape of the MOs.[1,6] Like dca, phenylcyanamide ion also exhibits π and σ orbitals of adequate energy, but as occurs in the azido bridge, phenylcyanamide is much more efficient in transmitting the magnetic interactions due to the higher electronic density in the coordinating N-atoms.

In a recent review about the phenylcyanamido ligands,[7] the poorly developed coordination chemistry of these ligands was pointed out by R. J. Crutchley, who indicated that their "coordination chemistry is expected to be as potentially rich as that of the pseudohalides azide or thiocyanate". This implies that, to date, complexes for most of the transition metals have not been reported. The most developed pcyd coordination chemistry is related to ruthenium cation, for which a large family of pcyd derivatives has been studied. But only structural information about several mononuclear ruthenium compounds,[7,8] three $(\mu$-pcyd$)_2$Ag^{I}, -Cu^{I}, and -Cu^{II} dinuclear complexes,[9] and some mononuclear Cu^{II}, Ni^{II}, Pd^{II}, and Mn^{II} compounds has been published,[10] together with nonstructurally characterized families of monomeric derivatives.[7] Another unexplored property of pcyd$^-$ anions is their behavior as superexchange mediators. To date, only the intriguing behavior of the closely related 1,4-phenyldicyanamido ligand has been studied from the magnetic point of view in dinuclear copper or ruthenium compounds.[7,11] These compounds show strong coupling between Ru^{III} centers separated by more than 13 Å, but magnetic properties for the $\mu_{1,3}$ and $\mu_{1,1}$ coordination modes of the pcyd$^-$ bridges have never been studied. In this sense, R. J. Crutchley indicates that "The ability of the dicyd^{2-} bridging ligands to mediate metal−metal coupling suggests that phenylcyanamide derivatives may find their way into molecular materials possessing useful electronic and/or magnetic properties".[7]

With the aim of exploring the magnetic and synthetic possibilities of this kind of ligand, we prepared several neutral [Mn(L$_2$)(X-pcyd)$_2$] derivatives in which the L$_2$ ligands are pyridinic ligands and the X-pcyd ligands are chloro- or fluoro-substituted phenylcyanamides. Successful syntheses and structural characterization have been carried out for several representative complexes, with formulas [Mn(H$_2$O)$_2$(4-bzpy)$_2$(3-Cl-pcyd)$_2$] (**1**), ($\mu_{1,3}$-3-Cl-pcyd)$_2$[Mn(2,2′-bpy)(3-Cl-pcyd)(MeOH)]$_2$ (**2**), ($\mu_{1,3}$-3-Cl-pcyd)$_2$[Mn(2,2′-bpy)(3-Cl-pcyd)(EtOH)]$_2$ (**3**), {($\mu_{1,3}$-4-Cl-pcyd)$_2$[Mn(2,2′-bpy)]}$_n$ (**4**), and [Mn(μ-4,4′-bpy)($\mu_{1,3}$-3-F-pcyd)$_2$]$_n$ (**5**), in which 4-bzpy is 4-benzoylpyridine, 2,2′-bpy and 4,4′-bpy correspond to 2,2′- and 4,4′-bipyridyl, and 3-Cl-pcyd, 4-Cl-pcyd, and 3-F-pcyd are the 3-chloro-, 4-chloro-, and 3-fluorophenylcyanamido ligands. These compounds were obtained by reaction in alcoholic medium of manganese salts and deprotonated phenylcyanamide in the presence of the corresponding pyridinic or bipyridinic ligands. The X-ray crystal structure determination reveals a wide variety of topologies and supramolecular arrangements: compound **1** is a mononuclear complex, but a net of hydrogen bonds gives a highly symmetric 2D network, compounds **2** and **3** are dinuclear complexes bridged by double phenylcyanamido ligands, giving supramolecular 1D systems by means of hydrogen bonds, compound **4** is a chain of manganese atoms linked by double phenylcyanamido bridges, and finally, compound **5** is a 2D system formed by the crossing of phenylcyanamido and 4,4′-bpy chains. Magnetic measurements for compounds **2**−**5** reveal a moderate AF coupling which lies in an intermediate position between the typical magnitudes of the couplings induced by $\mu_{1,3}$-azido and $\mu_{1,5}$-dicyanamido bridges. MO calculations on the free pcyd$^-$ anions and the main distortions in the bridging region point out the effect of the halo substituent in the *para* position, the chair distortion of the Mn−(NCN)$_2$−Mn unit, or the effect of the torsion of the phenyl rings on the superexchange interaction. The superexchange pathway has also been compared with those of related azido and dicyanamido ligands.

In the present paper we give the first structural data for polynuclear phenylcyanamide derivatives with Mn^{II}, the first examples of 1D or 2D systems derived from these ligands, and the first experimental variable-temperature susceptibility data and study as superexchange mediators for their $\mu_{1,3}$ coordination mode.

Experimental Section

Physical Methods. Magnetic susceptibility measurements were carried out on polycrystalline samples with a DSM8 pendulum susceptometer working in the range 4−300 K under magnetic fields of approximately 1 T. Diamagnetic corrections were estimated from the Pascal tables. The infrared spectra (4000−400 cm^{-1}) were recorded from KBr pellets on a Nicolet 520 FTIR spectrophotometer. EPR spectra were recorded with a Bruker ES200 spectrometer at X-band frequency. Thermogravimetric measurements were carried out in a Mettler TG 50 instrument at a heating rate of 10 °C·min^{-1}.

(7) Crutchley, R. J. *Coord. Chem. Rew*. **2001**, *219*−*221*, 125−155.
(8) Sondaz, E.; Gourdon, A.; Launay, J. P.; Bonvoisin, J. *Inorg. Chim. Acta* **2001**, *316*, 79.
(9) Brader, M. L.; Ainscough, E. W.; Baker, E. N.; Brodie, A. M. *J. Chem. Soc., Dalton Trans*. **1990**, 2785. Ainscough, E. W.; Baker, E. N.; Brader, M. L.; Brodie, A. M.; Ingham, S. L.; Waters, J. M.; Hanna, J. V.; Healy, P. C. *J. Chem. Soc., Dalton Trans*. **1991**, 1243. Ainscough, E. W.; Brodie, A. M.; Cresswell, R. J.; Turnbull, J. C.; Waters, J. M. *Croat. Chim. Acta* **1999**, *72*, 377.
(10) Crutchley, R. J.; Hynes, R.; Gabe, E. *Inorg. Chem*. **1990**, *29*, 4921. Letcher, R. J.; Zhang, W.; Bensimon, C.; Crutchley, R. J. *Inorg. Chim. Acta* **1993**, *210*, 183. Zhang, W.; Bensimon, C.; Crutchley, R. J. *Inorg. Chem*. **1993**, *32*, 580. Shen, X.; Shan, J.; Sun, H. B.; Kang, B. S. *J. Chin. Chem. Soc.* **1999**, *46*, 179.
(11) Aquino, M. A. S.; Lee, F. L.; Gabe, E. J.; Bensimon, C.; Greedan, J. E.; Crutchley, R. J. *J. Am. Chem. Soc*. **1992**, *114*, 5130. Cheruiyot, L. L.; Thompson, L. K.; Greedan, J. E.; Liu, G.; Crutchley, R. J. *Can. J. Chem*. **1995**, *73*, 573.

Table 1. Crystal Data and Structure Refinement for **1**−**5**

	1	**2**	**3**	**4**	**5**
empirical formula	$C_{38}H_{30}Cl_2MnN_6O_4$	$C_{50}H_{40}Cl_4Mn_2N_{12}O_2$	$C_{52}H_{44}Cl_4Mn_2N_{12}O_2$	$C_{24}H_{16}Cl_2MnN_6$	$C_{24}H_{16}F_2MnN_6$
MW	760.52	1092.62	1120.67	514.27	481.37
space group	$P2_1/a$	$P\bar{1}$	$P\bar{1}$	$I2/a$	$C2$
a, Å	7.630(3)	9.683(3)	10.684(4)	8.620(4)	17.276(9)
b, Å	12.559(5)	10.826(4)	11.980(5)	10.482(3)	11.599(6)
c, Å	18.886(7)	11.926(3)	12.003(5)	24.860(9)	10.646(6)
α, deg	90	88.71(2)	117.64(3)	90	90
β, deg	93.00(3)	77.04(3)	95.76(3)	99.45(4)	103.35(3)
γ, deg	90	83.16(3)	104.24(3)	90	90
V, Å^3	1807(1)	1209.7(7)	1277(1)	2215(1)	2075(2)
Z	2	1	1	4	4
T, °C	27	186	186	25	185
λ(Mo Kα), Å	0.71069	0.71069	0.71069	0.71069	0.71069
ρ_{calcd}, g·cm^{-3}	1.398	1.410	1.457	1.542	1.540
μ(Mo Kα), mm^{-1}	0.562	0.798	0.758	0.863	0.680
R1[a]	0.0473	0.0499	0.0439	0.0426	0.0473
ωR2[b]	0.1196	0.1425	0.1177	0.1256	0.1295

[a] $R1(F_o) = \sum F_o - F_c/\sum F_o$. [b] $wR2(F_o)^2 = \{\sum[w((F_o)^2 - (F_c)^2)^2]/\sum[w(F_o)^4]\}^{1/2}$.

Crystal Structure Determination and Refinement of the Structures. Crystal data and details of the structure determinations are presented in Table 1. Data were collected on a modified STOE four-circle diffractometer with graphite-monochromated Mo Kα radiation ($\lambda = 0.71069$ Å) and the ω-scan technique. The data of **1** and **4** were collected at room temperature and those of **2**, **3**, and **5** at −185(2) °C and processed in the usual way (corrections for Lp but not for absorption). The structures were solved by direct methods using the SHELXS-86 computer program[12] and refined by full-matrix least-squares methods on F^2, using the SHELXL-93 program[13] incorporated in the SHELXTL/PC V 5.03 program library[14] and the graphics program PLUTON.[15] All non-hydrogen atoms were refined anisotropically. Hydrogen atoms bonded to donor atoms were located from difference Fourier maps; the remaining ones were located on calculated positions by use of the HFIX utility of the SHELXL-93 program. Racemic twin refinement was applied in the case of **5**. Selected bond parameters are given in Tables 2−6 for compounds **1**−**5**, respectively.

Crystallographic data (excluding structure factors) for structures **1**−**5** have been deposited with the Cambridge Crystallographic Data Centre as supplementary publication nos. CCDC-185830 (**1**), -185831 (**2**), -185832 (**3**), -160794 (**4**), and 167320 (**5**). Copies of the data can be obtained free of charge on application to CCDC, 12 Union Rd., Cambridge CB2 1EZ, U.K. (fax, (+44) 1223-336-033; e-mail, deposit@ccdc.cam.ac.uk).

Synthesis. Neutral 3-fluoro-, 3-chloro-, and 4-chlorophenylcyanamide (X-pcyd-H), in all cases, were prepared by desulfurization of the corresponding X-phenylthiourea with lead acetate, following the general synthetic procedure described for the halo derivatives of phenylcyanamide.[16]

Compound **1** was prepared by reaction of a solution of manganese nitrate hexahydrate (1 mmol) and 4-benzoylpyridine (2 mmol) in 20 mL of methanol with a solution of 3-Cl-pcyd-H (2 mmol) in 5 mL of NaOH (0.2 M) to deprotonate the ligand. After the reagents were mixed, the resulting clear solution was allowed to evaporate, giving a yellow crystalline compound suitable for X-ray measurements in a few days. Yield: 42%. Anal. Calcd for $MnC_{38}H_{30}Cl_2N_6O_4$ (760.52): C, 60.0; H, 4.0; N, 11.1. Found: C, 59.9; H, 4.1; N, 11.2.

The method for compounds **2**−**4** was the same as that indicated for compound **1**, using 1 mmol of 2,2′-bpy instead of 2 mmol of 4-benzoylpyridine and using ethanol instead of methanol for compound **3**. The yields of the corresponding yellow products were 18%, 23%, and 51%, respectively. Anal. Calcd for **2**, $Mn_2C_{50}H_{40}Cl_4N_{12}O_2$ (1092.62): C, 55.0; H, 3.7; N, 15.4. Found: C, 54.5; H, 3.6; N, 15.3. Anal. Calcd for **3**, $Mn_2C_{52}H_{44}Cl_4N_{12}O_2$ (1120.67): C, 55.7; H, 3.9; N, 15.0. Found: C, 55.5; H, 3.8; N, 15.3. Anal. Calcd for **4**, $MnC_{24}H_{16}Cl_2N_6$ (514.27): C, 56.0; H, 3.1; N, 16.3. Found: C, 55.8; H, 3.2; N, 16.5.

Yellow crystals of compound **5** were obtained by a similar procedure using 4,4′-bpy instead of 2,2′-bpy. Yield: 20%. Anal. Calcd for $Mn_2C_{24}H_{16}F_2N_6$ (481.37): C, 59.9; H, 3.4; N, 17.5. Found: C, 59.6; H, 3.4; N, 17.5.

For compounds **1**−**3**, thermogravimetric analysis performed between 30 and 500 °C with a heating rate of 10 °C·min^{-1} shows well-defined losses of weight at moderate temperatures due to the coordinated solvents. For **1**, a 4.5% loss was observed at 130 °C (theoretical H_2O loss is 4.7%), followed by decomposition of the compound at temperatures higher than 150−160 °C. Compound **2** shows a loss of 5.6% due to the coordinated methanol molecules (theoretical MeOH loss is 5.85%) centered at 80 °C. After this first step the resulting compound is stable up to 300 °C. Compound **3** shows a loss of 8.3% due to the coordinated ethanol molecules (theoretical EtOH loss is 8.21%) centered at 85 °C. Decomposition of the resulting compound takes place at temperatures greater than 290 °C. Compounds **2** and **3** may lose coordinated solvent at room temperature when finely powdered samples are stored for several days. To avoid errors in the magnetic measurements, the corresponding samples were freshly extracted from the mother solutions, dried, and powdered just prior to the measurements being performed.

Results and Discussion

Infrared Spectra. Neutral pcyd-H shows a characteristic IR ν(NCN) stretching absorption in a low-wavenumber range (2225−2249 cm^{-1}), which shifts down to ca. 2120 cm^{-1} for deprotonated pcyd$^-$, suggesting a lower contribution of the resonance form containing the nitrile fragment. Nitrile-N-

(12) Sheldrick, G. M. *SHELXS-86, Program for the Solution of Crystal Structure*; University of Göttingen: Göttingen, Germany, 1986.
(13) Sheldrick, G. M. *SHELXL-93, Program for the Refinement of Crystal Structure*; University of Göttingen: Göttingen, Germany, 1993.
(14) *SHELXTL 5.03 (PC-Version), Program Library for the Solution and Molecular Graphics*; Siemens Analytical Instruments Division: Madison, WI, 1995.
(15) Spek, A. L. *PLUTON-92*; University of Utrecht: Utrecht, The Netherlands, 1992.
(16) Hollebone, B. R.; Nyholm, R. S. *J. Chem. Soc A* **1971**, 332.

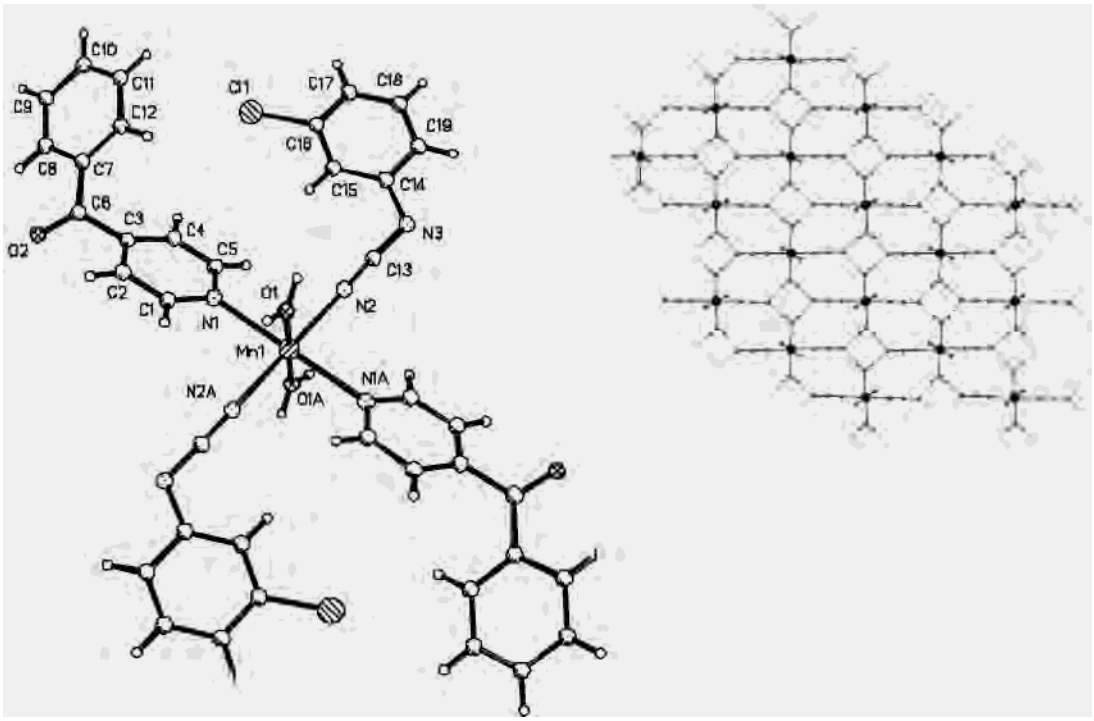

Figure 1. Labeled plot of **1** and the 2D supramolecular arrangement of compound **1** by means of H-bonds. Phenyl groups of the 4-Bzpy and 3-Cl-pcyd ligands have been omitted for clarity.

coordinated pcyd$^-$ ligands exhibit intermediate positions (always lower than 2200 cm^{-1}), with a dependence on the nature of the metallic center and the number of halo groups.[7] For the ligands used in this work, the ν(NCN) appears at 2239 cm^{-1} for 3-Cl-pcyd-H, 2238 cm^{-1} for 4-Cl-pcyd-H, and 2235 cm^{-1} for 3-F-pcyd-H. Coordination to Mn^{II} atoms shifts the signals down to 2154 cm^{-1} for 3-F-pcyd in compound **5** and 2133 cm^{-1} for 3-Cl-pcyd in compound **4** (only one kind of $\mu_{1,3}$-pcyd ligand). For 3-Cl-pcyd, the signal appears at 2160 cm^{-1} for **1** (only nitrile-N-coordinated pcyd ligands) and at 2155−2132 cm^{-1} for **2** and 2159−2133 cm^{-1} for **3** (containing the two $\mu_{1,3}$-pcyd and nitrile-N-coordinated pcyd coordination modes). These latter data indicate a criterion to differentiate the nitrile N coordination (2160−2155 cm^{-1} range) of the $\mu_{1,3}$ bridging mode, for which lower wavenumbers are found (2132−2133 cm^{-1}). Structurally characterized $\mu_{1,3}$ copper dimers agree reasonably with this assignation: ($\mu_{1,3}$-pcyd)$_2$[Cu(2,2′-bpy)(pcyd)$_2$]$_2$ also exhibits two similar absorptions at 2175 and 2103 cm^{-1}, whereas the Cu^I compound ($\mu_{1,3}$-4-Me-pcyd)$_2$[Cu(PPh$_3$)$_2$]$_2$ with only $\mu_{1,3}$-4-Me-pcyd ligands shows a single absorption at 2167−74 cm^{-1}.[9] The wavenumber sequence for the ν(NCN) stretching absorption seems then to be pcyd-H > $\mu_{1,3}$-pcyd > nitrile N coordination or anionic pcyd$^-$. These limited data referred to Mn^{II} derivatives suggest the above order, but further experimental data are required to obtain a general assignation.

Description of the Structure of [Mn(H$_2$O)$_2$(4-bzpy)$_2$(3-Cl-pcyd)$_2$] (1). This compound consists of centrosymmetric monomeric units in which the three different kinds of ligands adopt a *trans* arrangement around the central Mn^{II} ion, Figure 1. Bond distances are 2.145(2) Å between the Mn^{II} ion and the oxygen of the water molecules, a similar value of 2.154-(3) Å to the terminal N(2) of the cyanamido group, and a larger distance of 2.389(2) Å to the pyridinic N(1) atom of the 4-bzpy ligand, giving an elongated octahedron. Bond angles around the Mn atom are close to 90° in all cases. Monodentate phenylcyanamido ligand shows a linear coordination to the manganese atom with a Mn(1)−N(2)−C(13) bond angle of 179.0(3)°.

The linear −NCN unit is asymmetric with bond distances of N(3)−C(13) = 1.290(4) Å and C(13)−N(2) = 1.156(3) Å. The cyanamido unit is practically coplanar with the 3-Cl-phenyl group and shows a C(14)−N(3)−C(13) bond angle of 116.1(2)°. The most interesting feature of this structure lies in the moderately strong hydrogen bonds formed between the water molecules and N(3) nitrogen atoms from phenylcyanamido ligands of neighboring monomeric complexes, with N(3′)···O(1) distances of 2.856(4) and 2.843(4) Å and bond angles of 168(3)° for N(3′)−H(6)−O(1) and 167(2)° for N(3″)−H(7)−O(1). Each monomeric unit participates in four H-bonds, giving a supramolecular arrangement consisting of two-dimensional H-bonded layers, Figure 1. Selected bond parameters are given in Table 2.

Description of the Structure of ($\mu_{1,3}$-3-Cl-pcyd)$_2$[Mn(2,2′-bpy)(3-Cl-pcyd)(MeOH)]$_2$ (2). The structure consists of centrosymmetric dinuclear Mn units linked by double end-to-end 3-chlorophenylcyanamido bridges, Figure 2. The six coordination sites around the Mn atoms are occupied by one 2,2′-bpy ligand, one terminal nitrile atom of one 3-Cl-pcyd ligand, two bridging cyanamido ligands, and one solvent molecule (methanol). The linked 2,2′-bpy and the variety of ligands distort the coordination polyhedron of the Mn atom: bond angles range between 71.3(1)° for N(1)−Mn(1)−N(2) and 101.7(1)° for N(3a)−Mn(1)−N(5). The different natures of the N-atoms of the phenylcyanamido ligand also induce different bond parameters in the bridging region: Mn(1)−

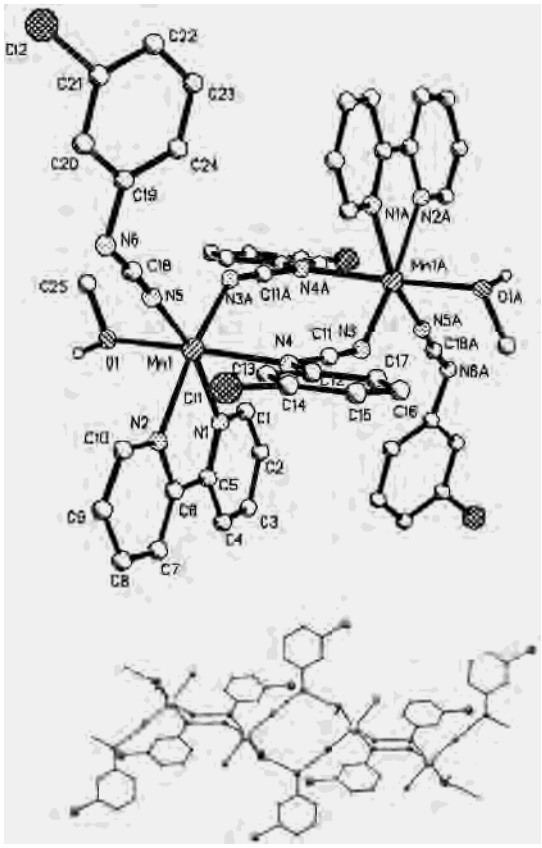

Figure 2. Labeled plot of **2** and the 1D supramolecular arrangement of compound **2** by means of H-bonds. Compound **3** shows an identical H-bond pattern.

Table 2. Selected Bond Lengths (Å) and Angles (deg) for **1**

Mn(1)−O(1)	2.145(2)	Cl(1)−C(16)	1.747(4)
Mn(1)−N(1)	2.389(2)	O(2)−C(6)	1.194(5)
Mn(1)−N(2)	2.155(3)	O(1)−H(6)	0.82(3)
N(2)−C(13)	1.155(4)	O(1)−H(7)	0.82(3)
N(3)−C(13)	1.290(4)		
N(3)−C(14)	1.410(4)		
O(1)−Mn(1)−N(1)	88.98(9)	Mn(1)−N(2)−C(13)	179.0(3)
O(1)−Mn(1)−N(2)	89.8(1)	N(2)−C(13)−N(3)	178.0(3)
O(1)−Mn(1)−O(1a)	180.00	C(13)−N(3)−C(14)	116.1(2)
O(1)−Mn(1)−N(1a)	91.02(9)	H(6)−O(1)−H(7)	112(3)
O(1)−Mn(1)−N(2a)	90.2(1)		
N(1)−Mn(1)−N(2)	93.12(9)		
N(1)−Mn(1)−N(1a)	180.00		
N(1)−Mn(1)−N(2a)	86.88(9)		
N(2)−Mn(1)−N(2a)	180.00		

N(4) takes a value of 2.291(2) Å, whereas Mn(1)−N(3a) is only 2.176(2) Å. Mn−N−C bond angles are also different, Mn(1)−N(4)−C(11) being 110.7(2)° in contrast with Mn(1)−N(3a)−C(11a), which takes a greater value of 140.3(2)°. As occurs in **1**, the monodentate phenylcyanamido ligands coordinate to the manganese atom in a quasi linear arrangement, with a Mn(1)−N(5)−C(18) bond angle of 172.3(2)°. The C−N−C angles between the cyanamido and the phenyl groups are similar for the terminal and bridging ligands: 118.5(3)° and 117.0(2)°, respectively. The Mn−$(NCN)_2$−Mn subunit shows a chair distortion similar to those often found in similar systems with double azido bridges.[1] This means that the two −NCN− groups are in the same plane with the manganese atoms placed 0.946(1) Å out of the main plane. The torsion angle between the plane determined by the two −NCN− groups and the N(4)−Mn(1)−N(3a) plane is 36.5°. The 3-Cl-pcyd ligand is practically planar with a minor torsion, C(13)−C(12)−N(4)−N(3), of 6.5°. The phenylcyanamido ligand is placed out of the main $(NCN)_2$ plane, which forms an acute angle of 28.6(2)° with the N(4)−C(12) bond direction. The shortest Mn···Mn intradimer distance is 5.292(1) Å.

Table 3. Selected Bond Lengths (Å) and Angles (deg) for **2**

Mn(1)−O(1)	2.216(2)	N(5)−C(18)	1.170(4)
Mn(1)−N(1)	2.319(3)	N(6)−C(18)	1.287(4)
Mn(1)−N(2)	2.270(3)	O(1)−H(26)	0.87(3)
Mn(1)−N(4)	2.291(2)	Cl(1)−C(14)	1.737(3)
Mn(1)−N(5)	2.142(3)	Cl(2)−C(21)	1.742(4)
Mn(1)−N(3a)	2.176(2)		
N(3)−C(11)	1.173(4)		
N(4)−C(11)	1.292(4)		
O(1)−Mn(1)−N(1)	89.11(9)	Mn(1)−N(4)−C(11)	110.7(2)
O(1)−Mn(1)−N(2)	88.20(8)	Mn(1a)−N(3)−C(11)	140.3(2)
O(1)−Mn(1)−N(4)	174.30(9)	Mn(1)−N(5)−C(18)	172.3(2)
O(1)−Mn(1)−N(5)	88.12(9)	C(11)−N(4)−C(12)	117.0(2)
O(1)−Mn(1)−N(3a)	89.13(9)	C(18)−N(6)−C(19)	118.5(3)
N(1)−Mn(1)−N(2)	71.27(10)	N(3)−C(11)−N(4)	176.1(3)
N(1)−Mn(1)−N(4)	85.57(9)	N(5)−C(18)−N(6)	175.5(3)
N(1)−Mn(1)−N(5)	164.8(1)		
N(1)−Mn(1)−N(3a)	93.2(1)		
N(2)−Mn(1)−N(4)	92.0(1)		
N(2)−Mn(1)−N(5)	93.7(1)		
N(2)−Mn(1)−N(3a)	164.26(9)		
N(3a)−Mn(1)−N(4)	89.1(1)		
N(3a)−Mn(1)−N(5)	101.7(1)		
N(4)−Mn(1)−N(5)	97.54(9)		

The dinuclear units generate a supramolecular one-dimensional H-bonded system by means of the −OH group of the coordinated methanol molecules and the N(6b) atoms of the terminal 3-Cl-pcyd ligands. Between each dinuclear unit appear two of these H-bonds, giving a structurally alternating 1D system, Figure 2. The N(6b)−O(1) distance is 2.699(4) Å, and the bond angle O(1)−H(26)−N(6b) takes a value of 167(4)°. Selected bond parameters are given in Table 3.

Description of the Structure of ($\mu_{1,3}$-3-Cl-pcyd)$_2$[Mn(2,2′-bpy)(3-Cl-pcyd)(EtOH)]$_2$ (3). The structure of this compound is similar to that of **2** by substitution of the coordinated methanol by one ethanol molecule, Figure 3. Bond parameters are very similar to those indicated for compound **2** in the ±2° range of difference. Phenylcyanamido ligands are also out of the main $(NCN)_2$ plane, which determines an acute angle of 23.9(1)° with the N(2)−C(2) bond direction.

As occurs for the above compound, dinuclear units are linked between them by double H-bonds between the N(4) atom of the terminal 3-Cl-pcyd ligand and the H-atom of the coordinated ethanol group, giving a one-dimensional supramolecular arrangement. The O(1)−N(4b) distance is 2.722(1) Å, and the O(1)−H(1)−N(4b) angle is 172(3)°. Selected bond parameters are given in Table 4.

Description of the Structure of {($\mu_{1,3}$-4-Cl-pcyd)$_2$[Mn(2,2′-bpy)]}$_n$ (4). The structure consists of a one-dimensional Mn system where the coordination environment around the Mn atoms includes one 2,2′-bpy ligand and four N-atoms of bridging 4-Cl-pcyd ligands.

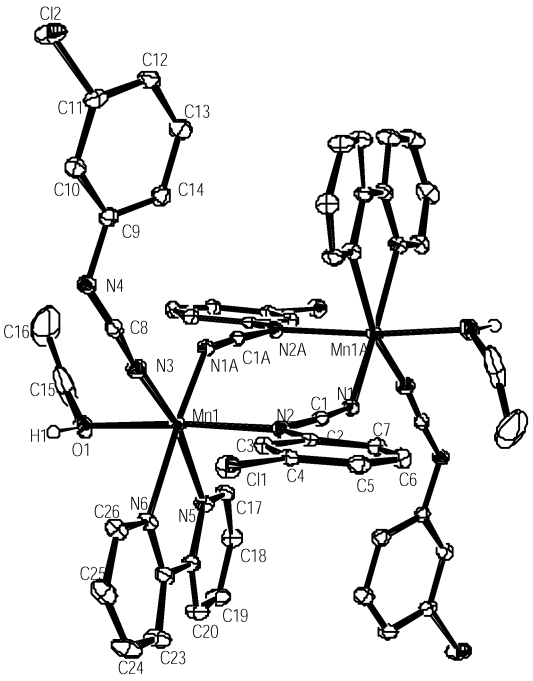

Figure 3. ORTEP plot of **3** with thermal ellipsoids at the 50% probability level.

Table 4. Selected Bond Lengths (Å) and Angles (deg) for **3**

Mn(1)−O(1)	2.209(2)	N(4)−C(9)	1.401(3)
Mn(1)−N(2)	2.291(3)	N(4)−C(8)	1.290(4)
Mn(1)−N(3)	2.146(3)	O(1)−H(1)	0.83(4)
Mn(1)−N(5)	2.302(3)	Cl(1)−C(4)	1.743(3)
Mn(1)−N(6)	2.297(2)	Cl(2)−C(11)	1.739(3)
Mn(1)−N(1a)	2.197(2)		
N(1)−C(1)	1.174(4)		
N(3)−C(8)	1.167(3)		
O(1)−Mn(1)−N(2)	172.14(9)	Mn(1)−N(2)−C(1)	111.9(2)
O(1)−Mn(1)−N(3)	90.08(9)	Mn(1a)−N(1)−C(1)	142.8(2)
O(1)−Mn(1)−N(5)	86.44(9)	Mn(1)−N(3)−C(8)	168.1(2)
O(1)−Mn(1)−N(6)	85.42(9)	C(1)−N(2)−C(2)	118.1(2)
O(1)−Mn(1)−N(1a)	90.03(9)	C(8)−N(4)−C(9)	118.2(2)
N(2)−Mn(1)−N(3)	97.78(9)	N(1)−C(1)−N(2)	175.0(3)
N(2)−Mn(1)−N(5)	85.95(9)	N(3)−C(8)−N(4)	176.5(3)
N(2)−Mn(1)−N(6)	94.06(9)		
N(1a)−Mn(1)−N(2)	88.62(9)		
N(3)−Mn(1)−N(5)	163.43(9)		
N(3)−Mn(1)−N(6)	91.94(9)		
N(1a)−Mn(1)−N(3)	101.46(9)		
N(5)−Mn(1)−N(6)	71.65(9)		
N(1a)−Mn(1)−N(5)	94.74(9)		
N(1a)−Mn(1)−N(6)	165.86(9)		

Double cyanamido bridges link the Mn atoms, giving a *cis* chain, Figure 4. The bond parameters in the bridging region show, in this case, similar bond lengths for Mn(1)−N(2), 2.253(2) Å, and Mn(1)−N(1b), 2.223(3) Å. However, as also occurs for the above compounds **2** and **3**, the bond angle Mn(1)−N(2)−C(1), 111.4(2)°, is clearly smaller than Mn(1)−N(1b)−C(1b), 140.4(2)°. The Mn−$(NCN)_2$−Mn subunit shows a chair distortion with the Mn atoms 0.964(1) Å out of the $(NCN)_2$ main plane and a dihedral angle of 36.8° between the N(1b)−Mn(1)−N(2) plane and the mean $(NCN)_2$ plane. In this case the deviation of the phenyl groups, given by the acute angle between the bond direction N(2)−C(2) and the $(NCN)_2$ plane is only 15.1(2)°. Mn···Mn intrachain distances are 5.328(1) Å, whereas the minimum

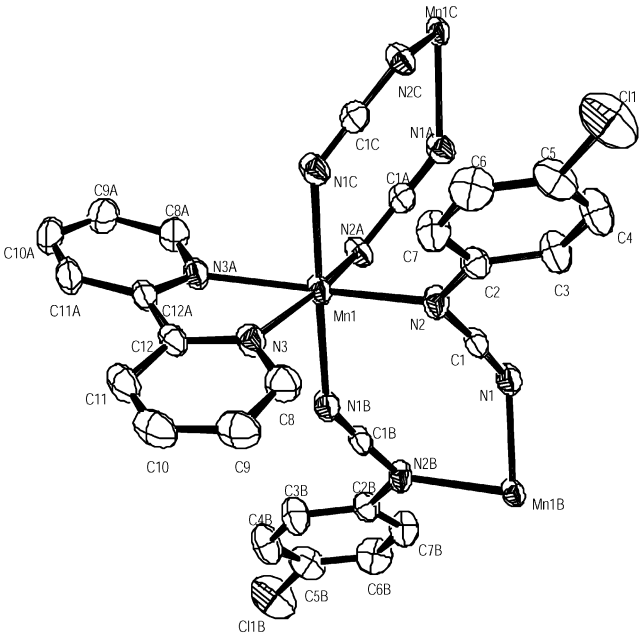

Figure 4. ORTEP plot of **4** with thermal ellipsoids at the 40% probability level.

Table 5. Selected Bond Lengths (Å) and Angles (deg) for **4**

Mn(1)−N(2)	2.253(2)	N(1)−C(1)	1.168(4)
Mn(1)−N(3)	2.284(3)	N(2)−C(1)	1.292(4)
Mn(1)−N(1b)	2.223(3)	Cl(1)−C(5)	1.746(3)
N(2)−Mn(1)−N(3)	97.22(9)	Mn(1b)−N(1)−C(1)	140.4(2)
N(2)−Mn(1)−N(2a)	94.94(9)	Mn(1)−N(2)−C(1)	111.4(2)
N(2)−Mn(1)−N(3a)	166.61(9)	C(1)−N(2)−C(2)	116.6(2)
N(2)−Mn(1)−N(1b)	88.2(1)	N(1)−C1−N(2)	176.2(3)
N(2)−Mn(1)−N(1c)	90.8(1)		
N(3)−Mn(1)−N(3a)	71.32(9)		
N(3)−Mn(1)−N(1b)	84.0(1)		
N(3)−Mn(1)−N(1c)	97.2(1)		
N(1b)−Mn(1)−N(1c)	178.47(9)		
N(1c)−Mn(1)−N(3a)	84.0(1)		

interchain Mn···Mn distance is 8.520(1) Å. The structures of compounds **2** and **3** closely approach that of compound **4**, by elimination of the solvent molecules. Selected bond parameters are given in Table 5.

Description of the Structure of [Mn(μ-4,4′-bpy)($\mu_{1,3}$-3-F-pcyd)$_2$]$_n$ (5). Substitution of the 2,2′-bpy by 4,4′-bpy determines a *trans* octahedral arrangement around the Mn atoms, Figure 5. The coordination sites around the manganese atom are occupied by two N-atoms of two bridging 4,4′-bpy ligands and by four bridging 3-F-pcyd ligands. Between the manganese atoms double cyanamido bridges determine a *trans*-3-F-pcyd−Mn chain. The structure may then be described as a two-dimensional system with 4,4′-bpy−Mn chains crossed by Mn−3-F-pcyd chains, Figure 5.

The bond parameters in the bridging region again show a clear difference between nitrile and amide N-atoms of the ligand: the bond lengths for Mn(1)−N(2) and Mn(2)−N(4) are 2.361(5) and 2.314(4) Å, whereas those for Mn(1)−N(3) and Mn(2)−N(1) are 2.179(4) and 2.189(5) Å, respectively. Bond angles related to the nitrile N-atom, Mn(1)−N(3)−C(8), 145.5(5)°, and Mn(2)−N(1)−C(1), 144.1(5)°, are larger than the angles related to the amide N-atom, Mn(1)−N(2)−C(1), 112.0(4)°, and Mn(2)−N(4)−C(8), 113.4(3)°. As

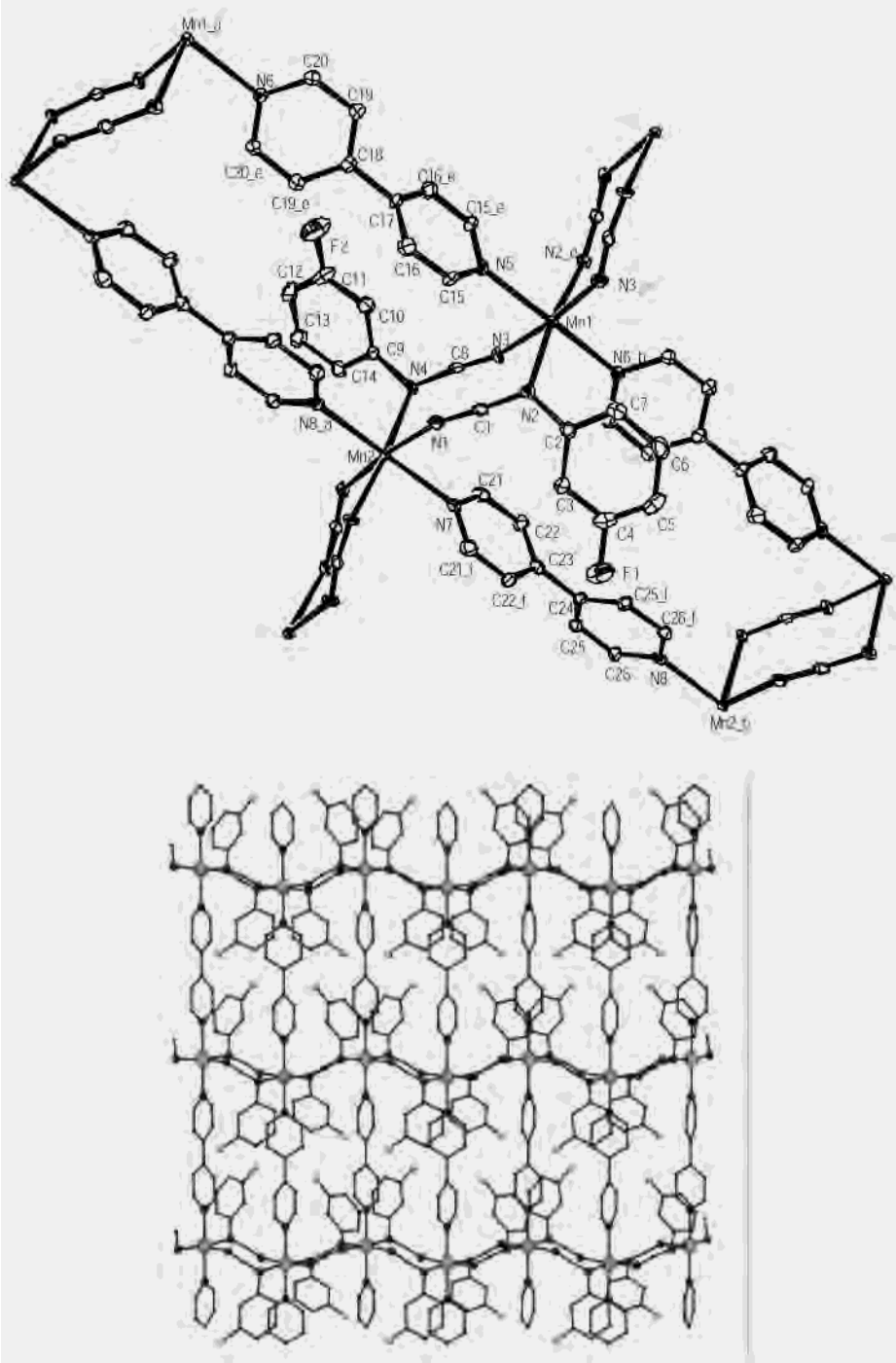

Figure 5. ORTEP plot of the basic unit of **5** with thermal ellipsoids at the 50% probability level and view of the 2D arrangement of **5** by means of the 3-fluorophenylcyanamido and 4,4′-bpy bridges.

occurs for the above compounds, Mn−$(NCN)_2$−Mn subunits show a clear chair distortion with the Mn atoms placed 0.730−0.750(1) Å out of the cyanamido plane. A dihedral angle of 27.7−27.0° is found between the $(NCN)_2$ plane and the N(2)−Mn(1)−N(3) or N(1)−Mn(2)−N(4) plane. Bridging phenylcyanamido ligands are far from planarity, showing torsion angles N(3)−N(4)−C(9)−C(10) of 40.5(4)° and N(1)−N(2)−C(2)−C(3) of 15.0(3)°.

In this case strong deviation of the 3-fluorophenyl groups is evidenced by the 45.9(4)° or 46.2(4)° acute angle between the bond direction N(4)−C(9) or N(2)−C(2) and the reference $(NCN)_2$ plane. The Mn···Mn distance in the cyanamido unit is 5.435(1) Å, that through the 4,4′-bpy bridge is 11.599(1) Å, and the minimum interplane Mn··· Mn distance is 10.404(1) Å. Selected bond parameters are given in Table 6.

Magnetic Measurements and Coupling Constant Calculation. Magnetic measurements were performed for compounds **1**−**5** in the 300−4 °C temperature range on freshly powdered crystalline samples (see the Experimental Section). Compound **1** shows a practically constant $\chi_M T$ value over the whole temperature range, indicating that the H-bond

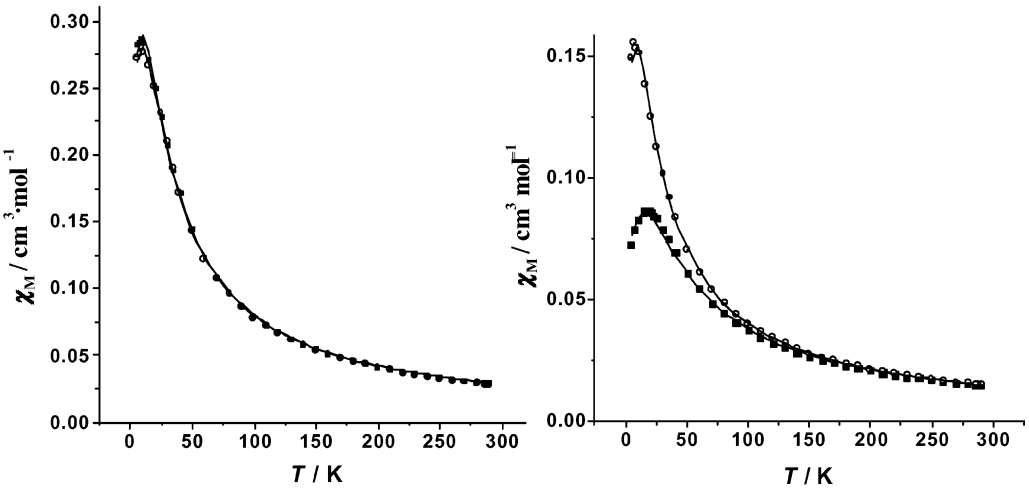

Figure 6. Susceptibility plots for compounds **2** and **3** (left) and for compounds **4** and **5** (right; **4**, filled squares; **5**, open circles).

Table 6. Selected Bond Lengths (Å) and Angles (deg) for **5**

Mn(1)−N(2)	2.361(5)	Mn(2)−N(1)	2.189(5)
Mn(1)−N(3)	2.179(4)	Mn(2)−N(4)	2.314(4)
Mn(1)−N(5)	2.279(8)	Mn(2)−N(7)	2.283(9)
Mn(1)−N(6b)	2.248(8)	Mn(2)−N(8a)	2.262(8)
N(1)−C(1)	1.165(7)	N(3)−C(8)	1.148(7)
N(2)−C(1)	1.292(7)	N(4)−C(8)	1.302(7)
F(1)−C(4)	1.351(8)	F(2)−C(11)	1.333(8)
N(2)−Mn(1)−N(3)	87.8(1)	N(1)−Mn(2)−N(4)	89.2(2)
N(2)−Mn(1)−N(5)	94.2(1)	N(1)−Mn(2)−N(7)	87.3(2)
N(2)−Mn(1)−N(6b)	85.8(1)	N(1)−Mn(2)−N(8a)	92.7(2)
N(2)−Mn(1)−N(2d)	171.5(2)	N(1)−Mn(2)−N(1e)	174.6(2)
N(2)−Mn(1)−N(3d)	92.6(1)	N(1)−Mn(2)−N(4e)	91.1(2)
N(3)−Mn(1)−N(5)	86.9(2)	N(4)−Mn(2)−N(7)	92.7(1)
N(3)−Mn(1)−N(6b)	93.1(2)	N(4)−Mn(2)−N(8a)	87.3(1)
N(3)−Mn(1)−N(2d)	92.6(1)	N(4)−Mn(2)−N(1e)	91.1(2)
N(3)−Mn(1)−N(3d)	173.9(2)	N(4)−Mn(2)−N(4e)	174.5(2)
N(5)−Mn(1)−N(6b)	180.00	N(7)−Mn(2)−N(8a)	180.00
N(5)−Mn(1)−N(2d)	94.2(1)	N(7)−Mn(2)−N(1e)	87.3(2)
N(5)−Mn(1)−N(3d)	86.9(2)	N(7)−Mn(2)−N(4e)	92.7(1)
N(2d)−Mn(1)−N(6b)	85.8(1)	N(4e)−Mn(2)−N(1e)	89.2(2)
N(2d)−Mn(1)−N(3d)	87.8(1)	N(4e)−Mn(2)−N(8a)	87.3(1)
N(3d)−Mn(1)−N(6b)	93.1(2)	N(1e)−Mn(2)−N(8a)	92.7(2)
Mn(1)−N(2)−C(1)	112.0(4)	Mn(2)−N(4)−C(8)	113.4(3)
Mn(1)−N(3)−C(8)	145.5(5)	Mn(2)−N(1)−C(1)	144.1(5)
C(1)−N(2)−C(2)	117.8(5)	C(8)−N(4)−C(9)	117.0(5)
N(1)−C(1)−N(2)	176.2(6)	N(3)−C(8)−N(4)	172.5(6)

network is not relevant at the magnetic level. For compounds **2**−**5** with their $\mu_{1,3}$-pcyd bridging groups, the overall interaction is moderately antiferromagnetic in all cases. The susceptibility plots for compounds **2** and **3** are practically identical, as may be expected from the similar bond parameters, Figure 6.

The susceptibility plots increase gradually on cooling and reach a maximum at 8 K for compound **2** and at 10 K for **3**. Best fit parameters obtained using the analytical expression derived from the isotropic Hamiltonian $H = -JS_1S_2$ were $J = -2.3(1)$ cm^{-1}, $g = 2.01(1)$ and $J = -2.3(2)$ cm^{-1}, $g = 2.01(1)$, respectively.

The magnetic susceptibility for compounds **4** and **5** also increases on cooling, reaching a broad maximum at 20 and 7 K, respectively, Figure 6. Coupling through the 4,4′-bpy bridges is negligible, so 2D compound **5** should be assumed as magnetically 1D through the cyanamido bridges. The experimental data were analyzed with the analytical expression for an isotropic $S = 5/2$ chain system[17] derived by Fisher from the Hamiltonian $H = \sum -JS_iS_{i+1}$; the best fit parameters were $J = -2.6(1)$ cm^{-1}, $g = 2.02(1)$ and $J = -1.4(1)$ cm^{-1}, $g = 2.03(1)$ for **4** and **5**, respectively.

The EPR spectra for compound **1** show an isotropic broad band with a peak-to-peak increment (Δ_{pp}) of 527 G at room temperature, centered at $g = 2.11$. Compounds **2** and **3** show similar features; between room temperature and 77 K the two compounds show one isotropic band centered at $g = 2.01$ with a Δ_{pp} of 254−270 G. At 4 K the spectra exhibit the main signal centered at $g = 2.02-2.03$ and a second weaker half-field band isotropically deplaced at $g = 5.15$ and 4.26, respectively. For compound **3,** two shoulders split symmetrically 760 G with respect to the central value of $g = 2.00$ appear clearly defined, reflecting weak anisotropy at very low temperature. The spectra of compounds **4** and **5** correspond nicely to that expected for 1D systems with moderate antiferromagnetic coupling and weak dipolar interactions (Mn···Mn distances around 5.5 Å).[18] Between room temperature and 77 K the isotropic signals centered at $g = 2.01$ show Δ_{pp} values of 74 and 85 G, respectively. We note that, for analogous Mn^{II}, doubly bridged chains with an end-to-end azido ligand with similar Mn···Mn intrachain distances have J values that typically lie around −10 cm^{-1}, the peak-to-peak line width being only 35 G due to the greater superexchange narrowing.[19] For weaker coupling, like that found in doubly dca bridged Mn^{II} chains, the peak-to-peak line width is much greater, reaching values around 100−120 G.[6] On cooling to 4 K, the isotropic bands show dipolar broadening with Δ_{pp} values of 275 and 328 G, respectively.

Superexchange Mechanism. Pcyd-bridged systems show evident similarities with the previously studied azido and dca, but the phenyl ring attached to the amide N-atom introduces an important number of variables which are not

(17) Fisher, M. E. *Am. J. Phys.* **1964**, *32*, 343.
(18) Bencini, A.; Gatteschi, D. *EPR of Exchange Coupled Systems*; Springer-Verlag: Berlin, Heidelberg, 1990; Chapter 10 and references therein.
(19) Abu-Youssef, M. A. M.; Escuer, A.; Gatteschi, D.; Goher, M. A. S.; Mautner, F. M.; Vicente, R. *Inorg. Chem.* **1999**, *38*, 5716.

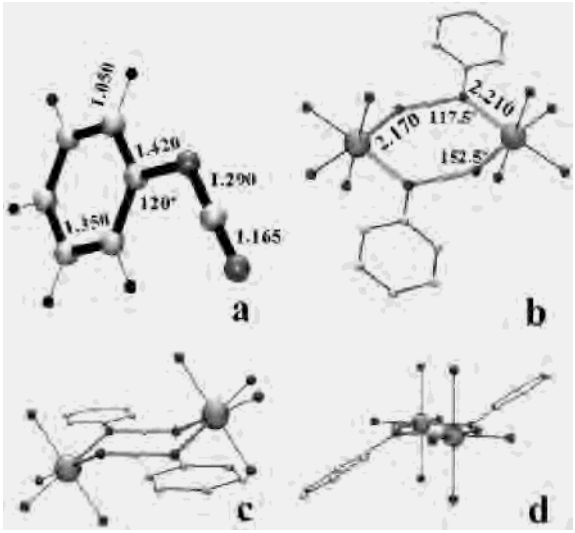

Figure 7. Scheme of the models used in the MO calculations. Other parameters assumed: F−C and Cl−C bond distances of 1.350 and 1.750 Å; remainder of the coordination sites around the Mn atoms as NH_3 ligands with a Mn−N bond distance of 2.100 Å.

Table 7. Δ Values for the Gaps between the Symmetric and Antisymmetric Combinations of the Pairs of Atomic Orbitals of the Metallic Centers with the Corresponding MOs of the Bridge and $\sum\Delta^2$ for Dinuclear Units Modeled As Shown in Figure 7b (Pcyd, 3-F-pcyd, 3-Cl-pcyd, and 4-Cl-pcyd), Figure 7c (Pcyd, Chair 30°), and Figure 7d (Pcyd, Rotated 25°)[a]

	$\Delta(x^2-y^2, d_{z^2})$	$\Delta(xz, yz)$	$\sum\Delta^2$
pcyd	0.295, 0.455	0.302, 0.319	0.487
3-F-pcyd	0.295, 0.454	0.307, 0.325	0.493
3-Cl-pcyd	0.295, 0.454	0.282, 0.291	0.458
4-Cl-pcyd	0.295, 0.454	0.542, 0.527	0.864
pcyd, chair 30°	0.095, 0.183	0.313, 0.281	0.220
pcyd, Ph rotation 30°	0.113, 0.263	0.291, 0.335	0.281

[a] The contribution of the d_{xy} orbitals (always lower than $\Delta = 0.02$ eV) has not been included.

present in the other ligands. Some of these factors are related to the distortions on the Mn−$(NCN)_2$−Mn unit (bond lengths and angles), derived from the asymmetric coordination of the nitrile and amide N-atoms or from the relative position of the phenyl rings and their halo groups. As an approach to the properties of the phenylcyanamido ligands as superexchange mediators, we have performed MO calculations with the CACAO program[20] for several ligands and complex distortions to evaluate the main factors that influence the superexchange mechanism. The calculations have been done on the models schematized in Figure 7 and using the indicated bond parameters. Hückel parameters were the standard of the program.

As a starting point, we calculated the MO diagram for the X-pcyd anions using the bond parameters indicated in Figure 7a, under C_s symmetry. The filled HOMOs are three π MOs and three σ MOs, Figure 8. The frontier MO is in all cases the same π 1a″ MO, with adequate electronic density in the NCN fragment overlapping with the adequate atomic orbitals of the metallic ions. The energy of this orbital increases following the sequence $pcyd^- < 3\text{-F-}pcyd^- < 3\text{-Cl-}pcyd^- \ll 4\text{-Cl-}pcyd^-$. The following MO corresponds to a σ 2a′ MO for $pcyd^-$ and $4\text{-Cl-}pcyd^-$ or a π 3a″ MO for 3-F- and $3\text{-Cl-}pcyd^-$. As can be seen in Figure 8, the 2a′ MO has two well-directed lobes in the metal−ligand bond direction, whereas 3a″ is practically a ring MO.

But this latter MO will not be relevant in the superexchange pathway due to the poor electronic density in the NCN region. It is relevant that despite this change in the HOMO order, the first σ 2a′ MO has practically the same energy for the four ligands. The ability of the following 4a′ MO as the superexchange pathway is strongly dependent on the C−N−M bond angle. In the compounds reported in this work, for which the bond angle between the manganese atom and the nitrile end of the bridge lies around 140−150°, the overlap should be negligible because the M−N bond direction corresponds to the nodal plane placed on the N atom, and then the 4a′ MO should be poorly useful in the superexchange interaction. The two lower 5a′ and 6a″ MOs, useful for shape and density in the NCN group, should give a lower contribution to the superexchange pathways due to their lower energy. From these data, we can conclude, in good agreement with partial previous calculations, that the relevant MOs involved in the superexchange pathways should be 1a″ and 2a′.[7,11] Each of these MOs is able to participate in two well-differentiated pathways: the 1a″ MO should be able to transmit some AF coupling by overlapping with atomic orbitals with a *z* component (*xz*, *yz*) of the metallic ions (π pathway), whereas 2a′ MO can overlap with the e_g atomic orbitals of the paramagnetic centers (mainly $d_{x^2-y^2}$), using the well-directed lobes in the Mn−N bond direction (σ pathway).

The next step was to perform MO calculations on a dimeric unit with a double X-pcyd bridge, modeled as shown in Figure 7b. In this case, the Mn−$(NCN)_2$–Mn unit and the position of the phenyl rings were assumed as rigorously coplanar. Analysis of the results was made following the Hay−Thibeault−Hoffmann formalism,[21] in which the antiferromagnetic component of the coupling constant *J* is related with the $\sum\Delta_i^2$ parameter, where each Δ_i is the gap between the symmetric and antisymmetric combinations derived from each atomic orbital of the paramagnetic centers. In this case, for a d^5 ion such as Mn^{II}, $\sum\Delta^2$ is the sum of five individual contributions. The result of the calculations is summarized in Table 7. As may be expected, the contribution to the superexchange mechanism due to the combinations of d_{xy} atomic orbitals is negligible, and the interactions are propagated by the two π and σ routes indicated above, one based in the $d_{x^2-y^2}$ or d_{z^2} atomic orbitals and the 2a′ MO of the bridge, and the other based in the π interaction of the 1a″ MO and the d_{xz} or d_{yz} atomic orbitals. From the data in Table 7, the contributions to the antiferromagnetic component of *J* should clearly be similar for the phenylcyanamido and 3-(chloro or fluoro)phenylcyanamido ligands. However, greater antiferromagnetic contribution to the antiferromagnetic component may be expected for the 4-Cl-pcyd bridging

(20) Mealli, C.; Proserpio, D. M. CACAO program (Computed Aided Composition of Atomic Orbitals). *J. Chem. Educ.* **1990**, *67*, 399.

(21) Hay, P. J.; Thibeault, J. C.; Hoffmann, R. *J. Am. Chem. Soc.* **1975**, *97*, 4884.

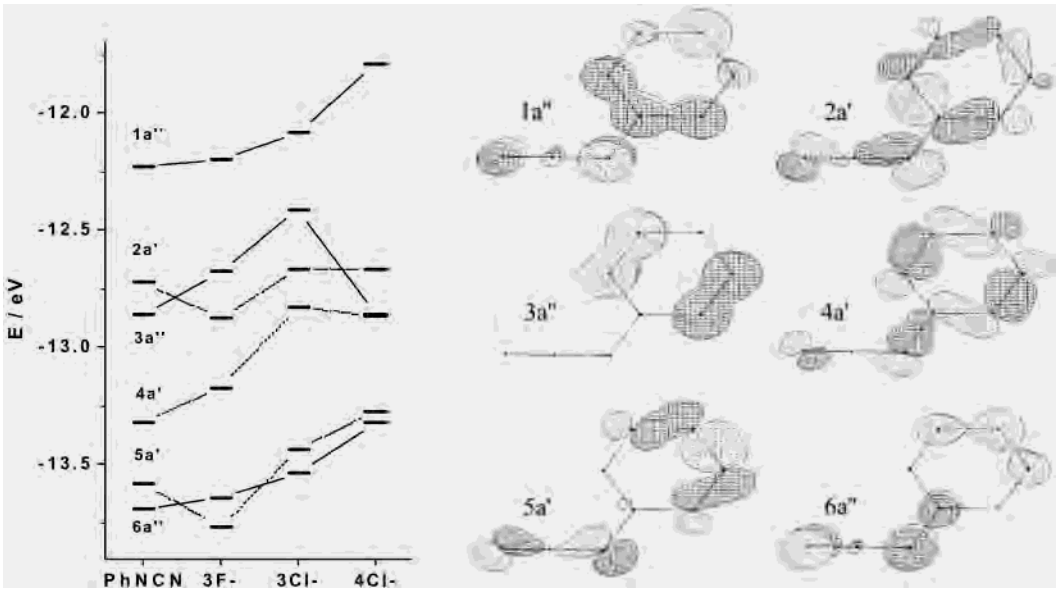

Figure 8. Left: energy levels for the set of three π (solid lines) and three σ (dotted lines) HOMOs of the X-pcyd ligands. Right: the six MOs potentially useful for the superexchange interaction (the main plane of the ligand placed in the *xy* plane).

ligand. This effect is directly related to the higher energy of the 1a″ HOMO orbital of 4-Cl-pcyd, which increases the relative energy of the corresponding antibonding MOs in the dimeric unit, increasing the efficiency of the π pathway. These results show that the positions of the halo groups can modify the coupling, whereas the electronegativity of the substituent seems less relevant.

The following calculations were devoted to the main distortions in the bridging region such as the planarity of the Mn−$(NCN)_2$–Mn unit and the relative positions of the phenyl rings. The first calculations were done on the dinuclear model shown in Figure 7c, where a chair distortion of 30° was introduced, maintaining the phenyl rings coplanar with the $(NCN)_2$ plane. As is reflected in Table 7, there is a drastic decrease of $\sum\Delta^2$ and then of the AF contribution, due mainly to the loss of overlap in the σ pathway. This result is very similar to that reported for the azido ligand, for which chair distortion in related doubly bridged azido systems is one of the most important factors that contribute to potential reduction of the AF coupling.[1]

Finally, the effect of the position of the phenyl rings was studied. One possible distortion is the loss of planarity by rotation along the amide N···ring C bond direction. Calculations were performed on the model schematized in Figure 7b, varying the dihedral angle between the X-phenyl ring and the main Mn−$(NCN)_2$–Mn plane, within the reasonable limits of ±30° (similar to the maximum deviation experimentally observed). In these limits, the results of the calculations shown as the loss of planarity of the ligand do not modify the magnitude of the coupling. In contrast, a significant decrease in the $\sum\Delta^2$ parameter is observed when the phenyl rings are placed 25° out of the Mn−$(NCN)_2$–Mn plane by rotation on the N−C−N axis as schematized in Figure 7d. From structural data, this kind of distortion is weak for **2** and **3** but important for **4** and **5**. As shown in Table 7, the torsion of the phenylcyanamido ligand out of the bridging plane reduces the contribution of the σ pathway. The reason may be easily envisaged as the loss of overlap due to the decreasing coplanarity between the e_g atomic orbitals and the 2a′ MO, which rotates out of the *xy* plane.

In conclusion, we may predict the following general rules for the $\mu_{1,3}$ coordination mode of $pcyd^-$ ligands.

(a) $Pcyd^-$ ligands are able to transmit moderate AF coupling between two paramagnetic centers using two clearly differentiated and equally important σ and π pathways for a d^5 system. Obviously, each pathway will be more or less relevant as a function of the electronic configuration of the paramagnetic center. Hence, the π pathway will be the only important one for a d^3 cation; the σ pathway will be the only important one for a d^8 or d^9 cation.

(b) Maximum AF coupling will be obtained for a planar arrangement of the atoms involved in the bridging region and phenyl groups. A decrease of the AF coupling will be obtained for chair distortion of the Mn−$(NCN)_2$–Mn bridging region.

(c) Greater AF coupling should be expected for 4-X-$pcyd^-$ ligands in comparison with $pcyd^-$ or 3-X-$pcyd^-$ bridging ligands.

(d) A decrease of the AF coupling will be obtained for systems in which the phenyl groups are out of the bridging plane by rotation along the NCN axis.

In our case, the above rules may be applied to compounds **4** and **5** for which the calculated *J* values show a drastic variation of 50% (-2.6 cm^{-1} for **4** and -1.4 cm^{-1} for **5**). The two compounds show similar bond environments in the bridging region and then similar a and b conditions. In contrast, following rule c, compound **4** (ligand 4-Cl-$pcyd^-$) should be more AF than **5** (ligand 3-F-$pcyd^-$). Also following rule d, compound **4** should be more AF coupled than **5** due to the larger NCN rotation of the phenyl rings (15.1° out of plane for **4** and around 46° out of plane for **5**). Experimentally, greater coupling corresponds to compound **4** in good agreement with the expected addition of both factors. Absolute comparison of the *J* values between compounds **4**

and **5** and **2** and **3** should be assumed with caution due to the different nuclearities of the systems, but for similar chair distortions and *m*-F or -Cl substitution, greater AF coupling was found for **2** and **3** in comparison with **5**, attributable to the lower out of plane rotation of the phenyl groups along the NCN axis.

A final comparison can be made for the azido, phenylcyanamido, and dicyanamido systems linked to Mn^{II} centers. From theoretical and experimental data, we can conclude that the efficiency of transmitting the superexchange interactions goes in the N_3^- > X-pcyd$^-$ ≫ $N(CN)_2^-$ order with typical values of the *J* parameter in 1D systems around −7/−15 cm^{-1} (azido), −1/−3 cm^{-1} (X-pcyd$^-$), and weaker than −0.5 cm^{-1} for dicyanamide. For the azido ligand the main superexchange pathway corresponds to the π interaction in the bridging *xy* plane with a comparatively lower contribution of the π overlap with the orbitals with a *z* component (*xz*, *yz*).[1] For the X-pcyd$^-$ ligands, the interaction through the σ (*xy*) pathway is reduced and is comparable with that through the π (*xz*, *yz*) pathway. However, for the $\mu_{1,5}$-dicyanamido ligand, both interactions are very weak and only the π (*xz*, *yz*) interaction is relevant.[6]

Acknowledgment. A.E., R.V., and N.S. thank the Ministerio de Ciencia y Tecnología (Spain), Project BQU2000/0791, for financial support of this research. F.A.M. thanks Prof. Belaj and Prof. Kratky (Technische Universität Graz) for the use of experimental equipment and OENB (Project 7967) for financial support.

Supporting Information Available: Listings of the final values of refined atomic parameters with esd's and bond lengths and angles in CIF format. This material is available free of charge via the Internet at http://pubs.acs.org.

IC025931L